sustainability

MDPI

Article

Spatio-Temporal Evolution Characteristics and Driving Factors of Typical Karst Rocky Desertification Area in the Upper Yangtze River

Weijie Gao, Siyi Zhou and Xiaojie Yin *

College of Forestry, Southwest Forestry University, Kunming 650233, China; gaoweijie@swfu.edu.cn (W.G.); siyi-Zhou@outlook.com (S.Z.)
* Correspondence: xjyinanne@163.com

Abstract: Karst rocky desertification (KRD) has become the most serious ecological disaster in the southwest of China and is a major obstacle to the sustainable development of the karst region in the southwest. Remarkably, scientific understanding of the spatial-temporal evolution of rocky desertification and the corresponding driving mechanism is the primary prerequisite crucial to controlling rocky desertification. Hence, the typical rocky desertification area of Qujing City, located in the upper reaches of the Yangtze River, was selected as the research object. On the basis of the Google Earth Engine (GEE) cloud platform and decision tree classification, the spatial-temporal evolution process of rocky desertification in Qujing City from 1990 to 2020 was investigated, and the driving factors of rocky desertification were explored in terms of the natural environment and socio-economic aspects. Consequently, over this period, the area of rocky desertification had decreased by 1728.38 km^2, while the no rocky desertification area had increased by 1936.61 km^2. Notably, the major driving factors of rocky desertification were fractional vegetation cover (FVC) (q = 0.41), land use type (q = 0.26), slope (q = 0.21), and land reclamation rate (q = 0.21). Typically, rocky desertification is likely to occur in areas with moderate or low FVC (<0.7), a low slope (0–8°) or high slope (35°–80°), a land type of cultivated-land or grassland, and a land reclamation rate of 10–70%. In addition, all two-factor interactions acted as drivers that exacerbate rocky desertification. Furthermore, FVC ∩ slope (q = 0.79) and slope ∩ land use type (q = 0.56) were two interacting drivers that promote rocky desertification strongly.

Keywords: upper Yangtze River; karst rocky desertification; space–time evolution; GEE; geographic detector; sustainable

Citation: Gao, W.; Zhou, S.; Yin, X. Spatio-Temporal Evolution Characteristics and Driving Factors of Typical Karst Rocky Desertification Area in the Upper Yangtze River. *Sustainability* **2024**, *16*, 2669. https://doi.org/10.3390/su16072669

Academic Editor: Antonio Miguel Martínez-Graña

Received: 29 January 2024
Revised: 13 March 2024
Accepted: 20 March 2024
Published: 25 March 2024

1. Introduction

The karst region in southwest China is the most typical subtropical karst concentration zone and has become one of the most serious areas of karst rock desertification (KRD) in the world [1,2]. Rocky desertification in the southwestern karst region has become a highly prominent regional environmental problem facing the ecological construction of China's western development and one of the primary obstacles to the sustainable development of southwest karst region [3–5]. The issue of rocky desertification is characterized by features such as exposed rocks, soil erosion, and reduced vegetation. This phenomenon not only directly impacts the stability of the local ecological environment, but also has severe consequences for soil and water conservation, as well as biodiversity. Specifically, research on the spatio-temporal evolution law of rocky desertification and its driving factors have become important prerequisites for the comprehensive treatment of rocky desertification and the restoration of the karst ecological environment [6,7].

The monitoring methods of rocky desertification mainly included human–computer interaction interpretation, supervision classification, spectral feature extraction, comprehensive analysis, quantitative extraction, and decision tree classification methods [8–10].

Compared to other methods, decision tree classification is a non-parametric classification method that is sensitive to spatial features and computationally efficient [11]. So, this technique has been widely utilized for remote sensing image classification. Nevertheless, previous studies seldom excluded areas, including non-karst environments, in which KRD will not occur, thus reducing the accuracy of KRD interpretations [12–14].

In the analysis of spatio-temporal changes in rocky desertification, the primary methods employed are temporal remote sensing monitoring and temporal trajectory remote sensing monitoring. Temporal remote sensing monitoring involves acquiring a series of temporally continuous satellite images to analyze seasonal and interannual variations in surface features, revealing long-term dynamic trends. Temporal trajectory remote sensing monitoring combines spatial and temporal information, recording surface changes in a trajectory format, providing more precise location tracking, and heightened sensitivity to short-term variations. To monitor the spatio-temporal changes in rocky desertification over an extended timeframe, this study utilized a time series analysis approach. By comparing rocky desertification data from different years, this research aimed to unveil the developmental processes and changing trends of rocky desertification.

Traditional mathematical analysis methods are usually employed to quantitatively analyze the driving factors, such as principal component analysis, regression analysis, analytic hierarchy process, factor analysis, superposition analysis, and Pearson's correlation coefficient method, etc. Nonetheless, the above-mentioned methods suffer from the problems of simplified reality and strong subjectivity, which make it difficult to investigate the spatial differentiation of factors and the interaction effect of multiple factors [15–17].

Qujing is located in the upper reaches of the Yangtze River and the source of the Pearl River, with an important ecological location. Unfortunately, the dramatic development of KRD seriously threatens the local ecological security [5,18–20]. The Third China Rocky Desertification Monitoring showed that the area of rocky desertification in Qujing is 42.67 thousand hectares, which highlights the long-term arduousness of the rocky desertification problem in this region. The severe rocky desertification issue in Qujing City has led to problems such as vegetation retrogression, soil erosion, and intensified conflicts between humans and the environment. This poses a significant threat to the ecological security of the upstream Yangtze River region, constraining the sustainable development of the local economy and the construction of an ecological civilization. Here, based on Landsat image data, Digital Elevation Model (DEM) data, and the geological map of Yunnan Province from 1990 to 2020, the KRD grade in the study region of Qujing City was classified using the Google Earth Engine (GEE) cloud platform with non-karst areas excluded. Specifically, the spatial and temporal evolution of regional rocky desertification was analyzed with remote sensing monitoring technology and a geographic detector, and its driving factors were further investigated. The achieved research results will provide decision support for government policymakers.

Therefore, the objectives of this study were as follows. (i) In utilizing the Google Earth Engine (GEE) cloud platform and employing the decision tree classification method to extract the distribution of different grades of rocky desertification, a map depicting the distribution of rocky desertification levels in Qujing City from 1990 to 2020 was generated. This aimed to explore the spatio-temporal evolution process of rocky desertification in Qujing City. (ii) Employ geographical detector techniques, including differentiation and factor detection, risk zone detection, ecological detection, and interaction detection, to analyze the relationship between rocky desertification and its driving factors. This study aimed to investigate the contribution rates of each factor, the contribution rates within factors, the spatial variability of factors, and the interactions among multiple factors.

2. Materials and Methods

2.1. Overview of the Research Area

Qujing City is located in the eastern part of Yunnan Province, with a latitude range of 24.34° N to 26.33° N and longitude range of 103.28° E to 105.89° E. The total area of

this city is 28,900 km^2, with 9 county-level administrative districts under its jurisdiction (Figure 1). The overall topography is dominated by plateau mountains, with widely distributed plateau basins, mountains, river valleys, and lake basins. In addition, the geological composition features carbonate rocks, mainly limestone and dolomite, resulting in the formation of typical karst landforms, including numerous caves, stone forests, and peak clusters. Moreover, Qujing City is characterized by six climate types, with a predominantly subtropical plateau monsoon climate. Generally, its annual average temperature is 14.3 °C, and the annual precipitation is 1038 mm. Despite its diverse natural geographical conditions, the situation of rocky desertification in Qujing City is still serious.

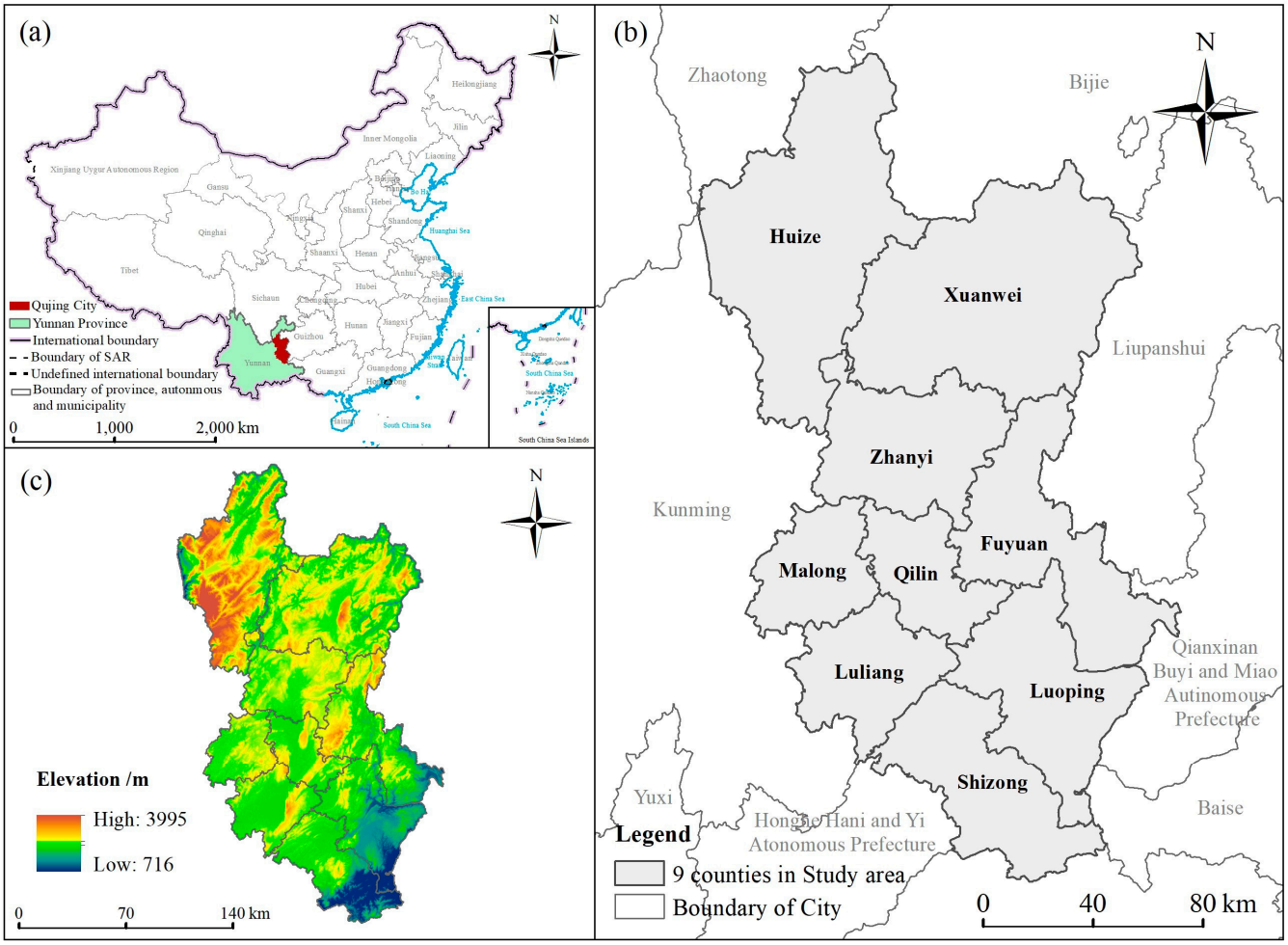

Figure 1. Administrative map of the study area: (**a**) location of study area in China, (**b**) map showing the 9 counties in the study area, (**c**) elevation distribution of the study area.

2.2. Research Data

2.2.1. Remote Sensing Data

Optical remote sensing data from Landsat satellites were employed, with Thematic Mapper (TM) data from 1990 to 2011 and Operational Land Imager (OLI) data from 2015 to 2020. In addition, the utilized remotely sensed data were acquired from the United States Geological Survey (USGS), and the corresponding specifications and acquisition dates are detailed in Table 1.

Table 1. Remote sensing image information.

Sensor	Remote Sensing Satellites	Year of Study	The Time Period for Compositing
TM	Landsat5	1990	1 January 1990–31 December 1990
TM	Landsat5	1995	1 January 1995–31 December 1995
TM	Landsat5	2000	1 January 2000–31 December 2000
TM	Landsat5	2006	1 January 2006–31 December 2006
TM	Landsat5	2011	1 December 2010–1 December 2011
OLI	Landsat8	2016	1 October 2015–1 October 2016
OLI	Landsat8	2020	1 January 2020–31 December 2020

Typically, the pre-processing of Landsat data mainly consists of de-cloud processing, image mosaicking, and study area cropping. Firstly, the Quality Assessment (QA) bands were filtered using the Landsat5 Surface Reflectance and Landsat8 Surface Reflectance provided by Google Earth Engine (GEE) to achieve the de-cloud processing. Subsequently, the annual image was synthesized by selecting one image per month from the year, making a total of 12 images, and using the mean value under the Reducer to composite these images into a single annual representation. Finally, the study area was extracted by clipping the synthesized image. Noteworthy, this study monitored the changes in rocky desertification in Qujing City from 1990 to 2020, and the target years were 1990, 1995, 2000, 2005, 2010, 2015, and 2020. In practice, after cloud processing, there were missing images for some years in the study area, so the target years were adjusted, and the final research periods were 1990, 1995, 2000, 2006, 2011, 2016, and 2020.

2.2.2. Environmental Factor Data

With reference to the relevant studies on the driving factors of rocky desertification, 11 factors were identified from the natural environment and socio-economic aspects for analyzing the driving factors of rocky desertification in the study area, which were selected in the year 2000, and the spatial resolution was uniformly re-sampled to 1 km × 1 km [21–24].

The slope and elevation data were extracted from DEM data acquired from the United States Geological Survey (USGS). In addition, data on annual average rainfall, soil type, and soil erosion were obtained from the Data Center for Resources and Environmental Sciences, Chinese Academy of Sciences "https://www.resdc.cn/" (accessed on 21 March 2023), with a spatial resolution of 500 m. Moreover, the soil types were derived from the spatial distribution data of soil types in China with a spatial resolution of 1 km. Additionally, the soil erosion came from the spatial distribution data of soil erosion in China with a spatial resolution of 1 km.

Population density and kilometer grid gross domestic product (GDP) data were obtained from the Data Center for Resources and Environmental Sciences of the Chinese Academy of Sciences "https://www.resdc.cn/" (accessed on 2 February 2023). Specifically, the population density data were obtained from the Chinese population spatial distribution kilometer grid data, with a spatial resolution of 1 km, and the kilometer grid GDP data were derived from the kilometer grid data set of China's GDP spatial distribution with a spatial resolution of 1 km. In addition, the GDP data of the primary industry were obtained from the China County (City) Social and Economic Statistical Yearbook 2001 on the China Economic and Social Big Data Research Platform "https://data.cnki.net/" (accessed on 2 February 2023). The data on land use type were acquired from the national geographic information resource directory service system "https://www.webmap.cn/main.do?method=index" (accessed on 2 February 2023), with a spatial resolution of 30 m. Furthermore, the land reclamation rate was extracted from the land use data of Qujing City.

In order to analyze the driving factors of rocky desertification in Qujing City, each factor was graded according to the current situation of the study area, and the grading criteria are shown in Table 2.

Table 2. Driving factors in karst rocky desertification.

Factor Type	Factor	Code	Divide into Hierarchies
Natural environmental factors	Slope	X1	0–5, 5–8, 8–15, 15–25, 25–35, 35–80 (unit: °)
	Elevation	X2	600–1200, 1200–1500, 1500–1800, 1800–2000, 2000–2200, 2200–2400, 2400–2900, 2900–4000 (unit: m)
	Average annual rainfall	X3	0–800, 800–900, 900–1000, 1000–1100, 1100–1200,1200–1300, 1300–1400, 1400–1500, 1500–1600, 1600–1700 (unit: mm)
	Soil types	X4	Yellow-brown soil, brown soil, dry laterite, red clay, new deposit, lime (rock) soil, purple soil, coarse bone soil, mountain meadow soil, paddy soil, red lateritic soil, red soil, yellow soil, rock, lake, reservoir
	FVC	X5	0–0.1, 0.1–0.2, 0.2–0.3, 0.3–0.4, 0.4–0.5, 0.5–0.6, 0.6–0.7, 0.7–0.8, 0.8–0.9, 0.9–1.0
	Soil erosion	X6	Microdegree, mild, moderate, intense, violent
Socioeconomic factors	Population density	X7	0–130, 130–180, 180–230, 230–300, 300–400, 400–1000(unit: people/km^2)
	Km grid GDP	X8	0–40, 40–60, 60–100, 100–150, 150–200, 200–600(unit: ten thousand CNY/km^2)
	GDP of primary industry	X9	0–3, 3–5, 5–7, 7–9, 9–11 (unit: billion)
	Land reclamation rate	X10	0, 0–10, 10–20, 20–30, 30–40, 40–50, 50–60, 60–70,70–80, 80–90, 90–100 (unit: %)
	Land use type	X11	Cultivated land, forest, grassland, other land

2.3. Methods

2.3.1. Classification of Rocky Desertification Levels

In taking into account the research results of other scholars and ecological environment standards, as well as the specific conditions of the study area, the FVC, rock exposure rate, and slope degree were selected as the indicators for the classification of rocky desertification [25–28]. The rocky desertification levels were categorized as follows: no rocky desertification, potential rocky desertification, mild rocky desertification, moderate rocky desertification, intense rocky desertification, and extremely intense rocky desertification. Potential rocky desertification refers to the tendency or trend of land to undergo rocky desertification in the future. That is, under certain natural and anthropogenic conditions, the land begins to show a trend toward rocky desertification but has not yet fully exhibited distinct characteristics of rocky desertification. In employing the GEE platform and based on normalization algorithms (Normalized Difference), the Normalized Difference Vegetation Index (NDVI) and Normalized Difference Rock Index (NDRI) were calculated [26]. The pixel binary model was used to calculate the fraction of vegetation cover (FVC) and the rock exposure rate (F_r) separately. Additionally, the slope was extracted from the DEM data. It is notable that the classification of rocky desertification levels adopts the decision tree classification method, featuring a non-parametric approach, which is sensitive to spatial features and has high computational efficiency and extensively used in the classification of remote sensing images [11], as detailed in Table 3. Non-karst areas were excluded from the geological map of Yunnan Province to derive the distribution map of rocky desertification in the study area.

1. The Normalized Difference Vegetation Index (NDVI) is currently the most widely used vegetation index, and it can effectively reflect the condition of land FVC and is extensively applied in the study of the stratification of rocky desertification [29].

$$NDVI = (NIR - RED)/(NIR + RED) \quad (1)$$

where *NIR* and *RED* represent the reflectance values in the near-infrared and red wavelength bands of the TM and OLI data, respectively.

Table 3. Standards for classifying rocky desertification.

Rocky Desertification Level	FVC	Rock Exposure Rate	Slope
No rocky desertification	0.8–1.0	0–0.2	0–5
Potential rocky desertification	0.7–0.8	0.2–0.3	5–8
Mild rocky desertification	0.5–0.7	0.3–0.5	8–15
Moderate rocky desertification	0.3–0.5	0.5–0.7	15–25
Severe rocky desertification	0.1–0.3	0.7–0.9	25–35
Extremely revere rocky desertification	0–0.1	0.9–1.0	35–90

Based on the pixel-based binary model, the FVC was calculated according to Equation (2):

$$FVC = (NVDI - NDVI_{veg}) / (NDVI_{veg} - NDVI_{soil}) \quad (2)$$

where $NDVI_{veg}$ refers to the NDVI value of regions completely covered by vegetation, and $NDVI_{soil}$ represents the NDVI value of an area with bare soil or without any FVC.

2. Rock exposure is the most direct external manifestation of rocky desertification, and the Normalized Difference Rock Index (NDRI) is particularly sensitive to exposed rocks that can effectively reflect the degree of rock exposure in the region [26].

$$NDRI = (SWIR2 - NIR) / (SWIR2 + NIR) \quad (3)$$

where *SWIR2* and *NIR* represent the reflectance values in the shortwave infrared 2 and near-infrared bands of the TM and OLI data, respectively.

Based on the pixel-based binary model, the rock exposure rate (F_r) was calculated according to Equation (4):

$$F_r = (NDRI - NDRI_{rock}) / (NDRI_{rock} - NDRI_{no}) \quad (4)$$

where $NDRI_{rock}$ denotes the NDRI value for an area completely exposed to rocks, and $NDRI_{no}$ represents the NDRI value for areas with no rock exposure at all.

Considering the effect of image noise in the practical research, the NDVI and NDRI values with cumulative frequencies of 95% and 5%, respectively, were selected as the maximum and minimum values.

2.3.2. Geographic Detector

The geographic detector was primarily employed to analyze the contribution rates of driving factors to the spatial distribution of rocky desertification and the interactions between various drivers, which comprises differentiation and factor detection, risk zone detection, ecological detection, and interaction detection [30].

1. Differentiation and Factor Detection

Through spatial heterogeneity, the consistency of the spatial distribution patterns between the dependent variable (rocky desertification) and independent variables (driving factors) can be detected. Moreover, the ability of the dependent variable to account for the independent variable (q-value) was further assessed. The *p*-value represents the level of statistical significance and serves as an indicator used to test the significance of the q-value. In hypothesis testing, when the *p*-value is less than the significance level (<0.01), it implies that the observed effect is statistically significant. Typically, q-value ranges from [0, 1], where larger values indicate that the factor has stronger explanatory power for the dependent variable. The calculation formulas are provided below:

$$q = 1 - \frac{\sum_{h=1}^{L} N_h \sigma_h^2}{N\sigma^2} = 1 - \frac{SSW}{SST} \quad (5)$$

$$SSW = \sum_{h=1}^{L} N_h \sigma_h^2,\ SST = N\sigma^2 \quad (6)$$

Here, h = 1, …, L denotes the stratum of variable Y or factor X, i.e., classification or partition. N_h and N refer to the number of cells in stratum h and the whole region, respectively. σ_h^2 and σ^2 represent the variances of Y values in stratum h and the whole region. *SSW* and *SST* are the sums of variances within the stratum (within sum of squares) and the total variance of the whole region (total sum of squares), respectively.

2. Risk Zone Detection

This focuses on the use of t-statistics to detect the strength of the combined impact of the various drivers of rocky desertification:

$$t_{\overline{y}_{h=1}-\overline{y}_{h=2}} = \frac{\overline{Y}_{h=1} - \overline{Y}_{h=2}}{\left[\frac{\mathrm{Var}\left(\overline{Y}_{h=1}\right)}{n_{h=1}} + \frac{\mathrm{Var}\left(\overline{Y}_{h=2}\right)}{n_{h=2}}\right]^{1/2}} \tag{7}$$

Here, $\bar{Y}_h$ represents the mean value of the attribute within subregion h, n_h denotes the sample size within subregion h, and *Var* represents the variance. The t-statistic approximately follows a Student's t-distribution. The larger the t-value, the greater the influence of the influencing factor on the spatial differentiation of rocky desertification. Notably, the null hypothesis *H0*: $\bar{Y}_{h=1} = \bar{Y}_{h=2}$ is rejected if there is a significant difference in the attribute means between two subregions at the confidence level σ.

3. Ecological Detection

The F-statistic was used to compare the effects of different combinations of driving factors on the spatial distribution of rocky desertification:

$$F = \frac{N_{X1}(N_{x2} - 1)SSW_{X1}}{N_{X2}(N_{x1} - 1)SSW_{X2}} \tag{8}$$

$$SSW_{X1} = \sum_{h=1}^{L1} N_h\sigma_h^2,\ SSW_{X2} = \sum_{h=1}^{L2} N_h\sigma_h^2 \tag{9}$$

Here, N_{X1} and N_{X2} represent the sample sizes of two factors $X1$ and $X2$, respectively. Moreover, SSW_{X1} and SSW_{X2} denote the sums of within-stratum variances formed by $X1$ and $X2$, respectively. $L1$ and $L2$ represent the number of strata for variables $X1$ and $X2$. The null hypothesis *H0:* $SSW_{X1} = SSW_{X2}$ is rejected if there is a significant difference in the effect of the interactions between factors $X1$ and $X2$ on the spatial distribution of attribute Y at the σ significance level.

4. Interaction Detection

This applies to testing whether multiple factors ($X1$, $X2$) have interactive effects. And the judgment criteria are as follows (Table 4):

Table 4. Discriminant method for detecting interaction effects.

Interaction Effect	Discrimination Method
Synergy	q($X1$∩$X2$) > q($X1$) or q($X2$)
Double synergy	q($X1$∩$X2$) > q($X1$) and q($X2$)
Nonlinear synergy	q($X1$∩$X2$) > q($X1$) + q($X2$)
Antagonism	q($X1$∩$X2$) < q($X1$) + q($X2$)
Single antagonism	q($X1$∩$X2$) < q($X1$) or q($X2$)
Nonlinear antagonism	q($X1$∩$X2$) < q($X1$) and q($X2$)

Within the context of this research, the dependent variable Y is the distribution of rocky desertification in 2000, i.e., the area of rocky desertification per square kilometer. The independent variables X includes 11 factors related to both the natural environment and socio-economic aspects. In addition, the independent variable X and the dependent variable Y were resampled to a uniform spatial resolution of 1 km × 1 km using ArcGIS, and values were extracted to generate a table. X and Y data were input into the geographic detector software to explore the relationship between rocky desertification and driving factors.

3. Results

3.1. Characteristics of Spatio-Temporal Distribution of KRD

From Figure 2, it can be observed that from 1990 to 2020, the overall pattern in the study area was dominated by potential rocky desertification and no rocky desertification, with a relatively small proportion of areas where rocky desertification had already occurred (mild, moderate, severe, and extremely severe). Typically, the rocky desertification regions were mainly concentrated in the northern and central parts of Qujing City, with a sporadic distribution in the southeastern part. Specifically, the northern part of Qujing City was characterized by a high degree of rocky desertification, with moderate, severe, and extremely severe rocky desertification concentrated in this area. In contrast, the central and southeastern parts showed a slight degree of rocky desertification, which was mainly manifested as moderate and mild rocky desertification. Overall, the spatial distribution of rocky desertification in Qujing City presented a trend of "light in the south and heavy in the north" pattern.

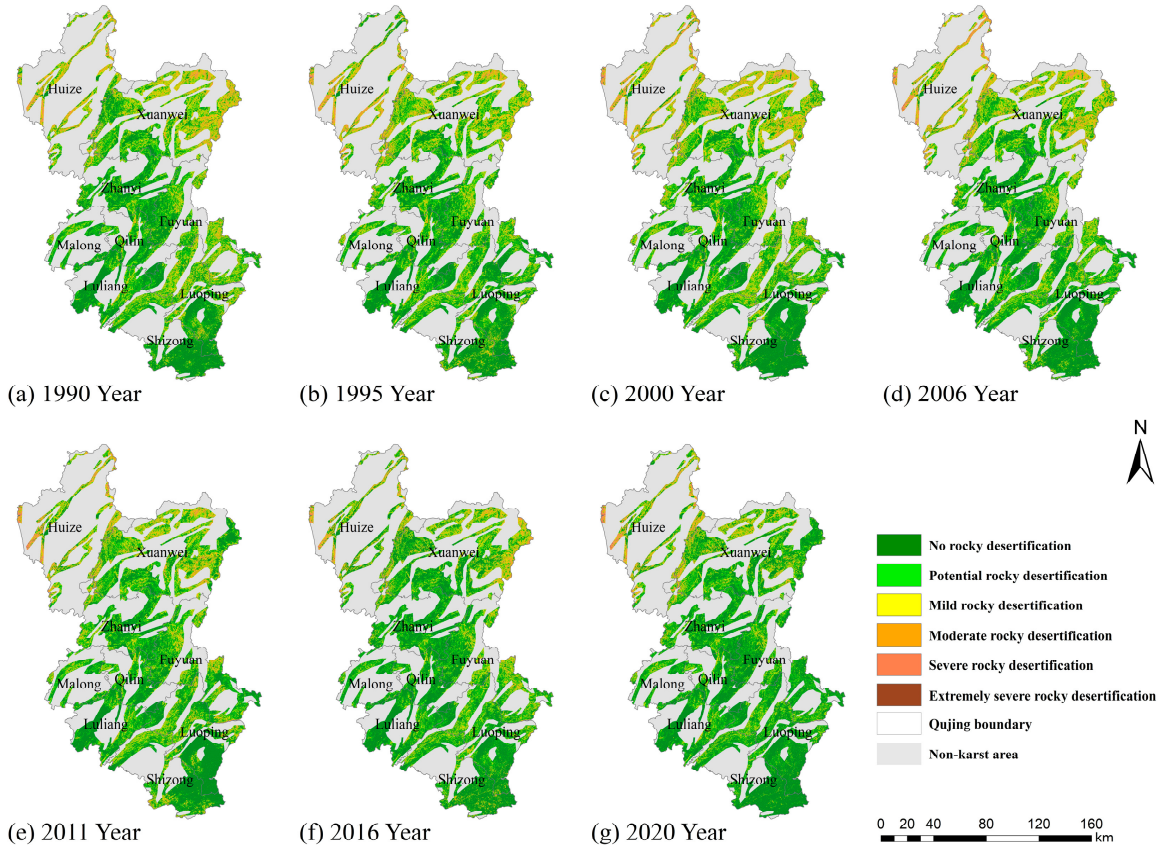

Figure 2. Rocky desertification grade distribution maps of Qujing from 1990 to 2020.

According to the results of rocky desertification grading from 1990 to 2020 in Qujing, the area of rocky desertification of each grade in 1990, 1995, 2000, 2006, 2011, 2016, and 2020 was counted, and the proportion was calculated (Table 5). From 1990 to 2020, the type of rocky desertification in Qujing City was dominated by potential rocky desertification and no rocky desertification, and the area of rocky desertification (mild, moderate, severe, and extremely severe) was relatively small. The area of rocky desertification decreased by 1728.38 km^2, while the area of no rocky desertification increased by 1936.61 km^2, accounting for 13.53%. This indicates that the overall condition of rocky desertification in Qujing City showed significant amelioration.

Table 5. Area dynamics of rocky desertification in Qujing from 1990 to 2020.

Year		No	Potential	Mild	Moderate	Severe	Extremely Severe
1990	Area/km^2	6565.45	2465.12	4052.36	1118.83	105.74	2.26
	Proportion/%	45.88	17.23	76.76	21.20	2.00	0.04
1995	Area/km^2	6595.45	2551.18	3999.18	1028.35	131.50	4.10
	Proportion/%	46.09	17.83	77.45	19.92	2.55	0.08
2000	Area/km^2	6591.89	2395.67	3916.08	1218.55	179.48	8.09
	Proportion/%	46.07	16.74	73.58	22.90	3.37	0.15
2006	Area/km^2	6955.89	2441.54	3706.78	1020.51	168.85	16.19
	Proportion/%	48.61	17.06	75.46	20.77	3.44	0.33
2011	Area/km^2	7162.65	2489.04	3601.97	918.06	128.60	9.44
	Proportion/%	50.05	17.39	77.33	19.71	2.76	0.20
2016	Area/km^2	7856.09	2320.47	3244.57	795.10	89.89	3.64
	Proportion/%	54.9	16.22	78.50	19.24	2.17	0.09
2020	Area/km^2	8502.06	2256.89	2786.29	648.71	108.39	7.42
	Proportion/%	59.41	15.77	78.47	18.27	3.05	0.21

From 1990 to 2020, the rocky desertification changes in each grade were relatively large in the rocky desertification area of Qujing City. In detail, the area of mild rocky desertification was always greater than 19%, and the area of moderate rocky desertification was 4–9%, while the area of severe and extremely severe rocky desertification was always less than 2%, indicating that the rocky desertification in Qujing City was mainly dominated by mild and moderate rocky desertification. From 1990 to 2020, the area of mild rocky desertification decreased continuously and decreased by 1266.07 km^2, accounting for 8.85% of the total area. Remarkably, the area of moderate rocky desertification showed a fluctuating downward trend, first decreasing (1990–1995), then increasing (1995–2000), and finally decreasing again (2000–2020). On the contrary, the area of intensely rocky desertification first increased, then decreased, and eventually increased again, reaching a peak in 2000.

Combined with the nine county-level administrative divisions of Qujing City, the change areas of no rocky desertification and rocky desertification during the 31-year period were counted, respectively. From 1990 to 2020, the areas without rocky desertification change were, in descending order, Xuanwei City, Fuyuan County, Luoping County, Shizong County, Qilin District, Huize County, Luliang County, Zhanyi District, and Malong District. Moreover, the areas of rocky desertification that decreased were, in descending order, Xuanwei City, Fuyuan County, Luoping County, Shizong County, Huize County, Qilin District, Zhanyi District, Luliang County, and Malong District. During the 31-year period, Xuanwei City experienced the greatest change in the areas of no rocky desertification and rocky desertification, which were 633.37 km^2 and 636.50 km^2, respectively, followed by Fuyuan County and Luoping County. On the contrary, Malong District recorded the smallest area of change with 9.09 km^2 and 7.80 km^2, respectively. This was because the total karst area in Xuanwei City, Fuyuan County, and Luoping County was among the top three in Qujing City, while the total karst area in Malong District was the least. Karst area was the basis for the occurrence and development of rocky desertification, and the rocky desertification area itself had a magnitude gap between administrative regions, which limited the variability of the rocky desertification area in Malong District, indicating that there was no rocky desertification, and therefore, the rocky desertification area had the least variability.

3.2. Analysis of Driving Factors of Rocky Desertification in Qujing City

3.2.1. Influence Analysis

The contribution rate of driving factors to the spatial distribution of rocky desertification was analyzed through differentiation and factor detection (Table 6). Notably, the *p* value of all driving factors was less than 0.01, indicating that the q value of all driving

factors was significantly different. Therefore, the contribution rates of all 11 factors were analyzed. The effects of natural environmental factors on the spatial distribution of rocky desertification in Qujing City were in the following order: FVC (q = 0.41) > slope (q = 0.21) > elevation (q = 0.11) > average annual rainfall (q = 0.07) > soil type (q = 0.05) = soil erosion (q = 0.05). Moreover, the impacts of socio-economic factors on rocky desertification were ranked as follows: land use type (q = 0.26) > land reclamation rate (q = 0.21) > gross domestic product of primary industry (q = 0.06) = population density (q = 0.06) > GDP per kilometer grid (q = 0.01). According to the definition of the q value, among the six natural environmental factors, the FVC and slope were the main driving factors of rocky desertification; among the five socio-economic factors, the land use type and land reclamation rate were the main driving factors.

Table 6. Effects of different driving factors on rocky desertification.

ActuateDivisor	Natural Environmental Factors					Socio-Economic Factors					
	X1	**X2**	**X3**	**X4**	**X5**	**X6**	**X7**	**X8**	**X9**	**X10**	**X11**
q	0.21	0.11	0.07	0.05	0.41	0.05	0.06	0.01	0.06	0.21	0.26
p	<0.01	<0.01	<0.01	<0.01	<0.01	<0.01	<0.01	<0.01	<0.01	<0.01	<0.01

By comparing the q values of natural environmental factors with socio-economic factors, FVC was identified as the largest natural factor. The average q value of natural factors (0.15) exceeded that of socio-economic factors (0.12). This suggests that natural environmental factors had a greater impact on the occurrence and development of rocky desertification than socio-economic factors in Qujing City.

3.2.2. Risk Analysis

Risk zone detection was used to recombine the attribute values of the internal division of a single factor and analyze the effect of the combination on the spatial distribution of rocky desertification. According to the factor detection, the main driving factors of rocky desertification in Qujing City were the FVC, land use type, slope, and land reclamation rate. Therefore, the risk zone detection was analyzed for the above-four main driving factors.

According to Table 7, the higher the value of FVC combination, the lower the impact on rocky desertification, i.e., rocky desertification is less likely to occur in areas with a high FVC (>0.7). Consequently, the combination of a low FVC (<0.7) played a dominant role in the spatial distribution of rocky desertification, which was consistent with the ecology of rocky desertification areas in reality.

Table 7. Effects of different FVC combinations on rocky desertification (Confidence level: 0.05).

FVC	0–0.1	0.1–0.2	0.2–0.3	0.3–0.4	0.4–0.5	0.5–0.6	0.6–0.7	0.7–0.8	0.8–0.9	0.9–1
0–0.1										
0.1–0.2	Y									
0.2–0.3	Y	Y								
0.3–0.4	Y	Y	Y							
0.4–0.5	Y	Y	Y	Y						
0.5–0.6	Y	Y	Y	Y	Y					
0.6–0.7	Y	Y	Y	Y	Y	Y				
0.7–0.8	Y	Y	Y	Y	Y	Y	Y			
0.8–0.9	Y	Y	Y	Y	Y	Y	Y	N		
0.9–1	Y	Y	Y	Y	Y	Y	N	N	N	

Note: Y: There is a significant difference; N: There is no significant difference.

As shown in Table 8, except for the combination area with slopes of 25°–35°, 15°–25° and 8°–15°, other slope ranges had a significant impact on rocky desertification. This is because human activities are more frequent and intensive in low-slope areas (0–5°, 5°–8°),

while rocky desertification is more likely to occur in high-slope areas (35°–80°) where the natural ecological environment is poor.

Table 8. Effects of different slope combinations on rocky desertification (Confidence level: 0.05).

Slope	0–5°	5°–8°	8°–15°	15°–25°	25°–35°	35°–80°
0–5°						
5°–8°	Y					
8°–15°	Y	Y				
15°–25°	Y	Y	Y			
25°–35°	Y	Y	N	N		
35°–80°	Y	Y	Y	Y	Y	

Note: Y: There is a significant difference; N: There is no significant difference.

Based on Table 9, it is clear that except forest land and other land uses, other land use types have a significant impact on rocky desertification. This may be due to the fact that the forest land types (including forest land, shrubland, and sparse forest land) and other land types (including marshland and bare land) significantly increased the uncertainty of the occurrence and development of rocky desertification. As a result, special attention should be paid to the formulation of ecological restoration policies according to local conditions in future work on rocky desertification prevention and control, and no generalizations should be made.

Table 9. Effects of different land use type combinations on rocky desertification (Confidence level: 0.05).

Land Use Type	Plowland	Forest Land	Meadow	Other Land
plowland				
Forest land	Y			
meadow	Y	Y		
Other land	Y	N	Y	

Note: Y: There is a significant difference; N: There is no significant difference.

The land reclamation rate in this study was calculated as the proportion of cultivated land area per square kilometer. Hence, a land reclamation rate of 0 means that a square kilometer of land is not cropland and may therefore be forest or another type of land. When the land use type is forest land, it can be categorized into forest land, shrubland, or sparse forest land depending on the density of the canopy. Notably, the occurrence probability of rocky desertification is different for each forest land type. Moreover, the possibility of rocky desertification is also varied within the context of other land use types. As a result, the uncertainty of rocky desertification increases considerably when the area of cultivated land per square kilometer is too small, and the results show that there is no significant difference between the land reclamation rate of 0 and the combination of 0–10% (Table 10). Conversely, a high rate of land reclamation indicates good soil conditions and is largely free of rocky desertification. Therefore, there was little difference between the combinations having high rates of land reclamation, as shown in Table 10.

Table 10. Effects of different land reclamation rate combinations on rocky desertification (Confidence level: 0.05) (%).

Land Reclamation Rate	0	0–10	10–20	20–30	30–40	40–50	50–60	60–70	70–80	80–90	90–100
0											
0–10	N										
10–20	Y	Y									
20–30	Y	Y	Y								

Table 10. *Cont.*

Land Reclamation Rate	0	0–10	10–20	20–30	30–40	40–50	50–60	60–70	70–80	80–90	90–100
30–40	Y	Y	Y	Y							
40–50	Y	Y	Y	Y	Y						
50–60	Y	Y	Y	Y	Y	Y					
60–70	Y	Y	Y	Y	Y	Y	Y				
70–80	Y	Y	Y	Y	Y	Y	Y	Y			
80–90	Y	Y	Y	Y	Y	Y	Y	N	N		
90–100	Y	Y	Y	Y	Y	Y	Y	N	N	N	

Note: Y: There is a significant difference; N: There is no significant difference.

3.2.3. Difference Analysis

Ecological detection was employed to compare whether there is a significant difference between the combination of two factors on rocky desertification. Table 11 shows that the combination of the main driving factors of rocky desertification exhibits significant differences on the spatial distribution of rocky desertification, indicating that the interaction between the main driving factors has a great impact on the occurrence and development of rocky desertification. Nevertheless, the effects of the five factors, including the annual average rainfall, soil type, soil erosion, population density, and gross domestic product of primary industry, on rocky desertification did not differ significantly between any two of the factors, and therefore, the combination of these factors was not further analyzed for their interactions.

Table 11. Effects of different combinations of driving factors on rocky desertification (Confidence level: 0.05).

Actuate Divisor	X1	X2	X3	X4	X5	X6	X7	X8	X9	X10	X11
X1											
X2	Y										
X3	Y	Y									
X4	Y	Y	N								
X5	Y	Y	Y	Y							
X6	Y	Y	N	N	Y						
X7	Y	Y	N	N	Y	N					
X8	Y	Y	Y	Y	Y	Y	Y				
X9	Y	Y	N	N	Y	N	N	Y			
X10	N	Y	Y	Y	Y	Y	Y	Y	Y		
X11	Y	Y	Y	Y	Y	Y	Y	Y	Y	Y	

Note: Y: there is a significant difference, N: there is no significant difference. X1: slope; X2: altitude; X3: average annual rainfall; X4: soil type; X5: FVC; X6: soil erosion; X7: population density; X8: km grid GDP; X9: gross product of primary industry; X10: land reclamation rate; X11: land use type.

3.2.4. Interaction Analysis

In reality, the occurrence and development of rocky desertification is the result of the interaction of multiple factors. Hence, the interaction between different environmental factors was studied and the specific type of interaction between two factors was assessed based on the interaction detection of the geo-detector. In comparing the q-value of two factors with the q-value under the interaction, the latter has a larger q-value, indicating that the interaction of the two factors enhances the explanatory power of rocky desertification, otherwise the explanatory power under the interaction is weakened.

According to Table 12, the interactive driving factors with high explanatory power on the spatial distribution of rocky desertification in Qujing City are FVC ∩ slope (q = 0.79) and slope ∩ land use type (q = 0.56). Among the natural environmental factors, FVC ∩ slope (q = 0.79) and FVC ∩ average annual rainfall (q = 0.45) showed greater explanatory

power for rocky desertification in the interaction of the two factors. While among the socio-economic factors, land use type ∩ gross value of primary industry production (q = 0.33) and land use type ∩ land reclamation rate (q = 0.32) exhibited greater explanatory power. Moreover, in the interaction between natural factors and social factors, slope ∩ land use type (q = 0.56) and FVC ∩ land reclamation rate (q = 0.49) possessed greater explanatory power. Consequently, the interaction between natural factors (vegetation cover ∩ slope) was greater than the interaction between social and natural factors (slope ∩ land use type), and is even greater than the interaction between social factors (land use type ∩ GDP of the primary industry). This also indicates that the explanatory power of natural environmental factors in the spatial distribution of rocky desertification in Qujing City is more significant.

Table 12. Interaction of different driving factors on rocky desertification (q value).

Actuate Divisor	X1	X2	X3	X4	X5	X6	X7	X8	X9	X10	X11
X1	0.21										
X2	0.39	0.11									
X3	0.31	0.18	0.07								
X4	0.27	0.15	0.14	0.05							
X5	0.79	0.43	0.45	0.44	0.41						
X6	0.27	0.15	0.11	0.10	0.42	0.05					
X7	0.31	0.16	0.17	0.11	0.42	0.11	0.06				
X8	0.23	0.16	0.15	0.08	0.45	0.07	0.13	0.01			
X9	0.29	0.20	0.18	0.11	0.47	0.11	0.11	0.07	0.06		
X10	0.40	0.30	0.30	0.26	0.49	0.25	0.26	0.23	0.27	0.21	
X11	0.56	0.32	0.32	0.29	0.47	0.28	0.30	0.29	0.33	0.32	0.26

The q values for the interactions of FVC ∩ slope, land use type ∩ primary industry product, and slope ∩ land use type were all greater than the sum of the q values of the respective two factors, indicating that the relationship between each two factors was nonlinearly enhanced. In addition, the q values for the interactions of FVC ∩ average annual rainfall, land use type ∩ land reclamation rate, and FVC ∩ land reclamation rate were all larger than that of any one factor, indicating that there was a two-factor enhancement relationship between each of the two factors. Although the q values of the interaction of each environmental factor were different, they were all greater than that of a single factor, and the interaction between the factors acted as facilitators.

4. Discussion

4.1. Methodological Capabilities and Limitations

The extraction of rocky desertification information is based on remote sensing technology, which is better than using the Environment for Visualizing Images (ENVI) to simulate the distribution of rock desertification grades. In previous studies, the periods chosen were mostly January–April and November–December to minimize the impact of bare rock by FVC, but during these periods, there was less vegetation on the surface of the cultivated land, which increased the likelihood of a misclassification of rocky desertification grades. In addition, in some studies, non-karstic areas are not excluded from the classification of rocky desertification [31], resulting in one-sided results. In this study, the GEE cloud platform was used to grade the intensity of rocky desertification in Qujing City from 1990 to 2020. Significantly, a whole image of each year was integrated to avoid the problem of a small FVC caused by the selection of data in some years, and consequently, the temporal and spatial changes in rocky desertification could be analyzed and studied.

In this study, when analyzing the driving factors of karst rocky desertification, we encountered some challenges in the data collection and processing. Notably, economic indicators such as the GDP of primary industries, calculated on the basis of county-level administrative units, could be significantly affected by changes in administrative divisions.

Moreover, the geo-detector model we used was mainly based on the type and quantity of point data, introducing certain errors in the analysis of the contribution rate of driving factors for rocky desertification in large-scale regions. These errors stem from the conversion of spatial scales, inconsistencies in the data integration process, and the accumulation of errors between different data sources. However, it is important to emphasize that the original data relied upon in this study came from national authoritative institutions and scientific research databases, such as the Data Center for Resources and Environmental Sciences, Chinese Academy of Sciences, and the United States Geological Survey (USGS). These data sources, providing remote sensing images and socio-economic data, have been validated over many years and are widely recognized for their high reliability and accuracy. Although errors may be introduced in the data processing and model analysis process, by selecting authoritative data sources and using mature analysis methods, the accuracy and reliability of the research results were maximized to the greatest extent.

This study considered data only from the year 2000, primarily due to the availability of the data, which limited the exploration of era-specific changes in the impact of the driving factors. Future research should extend to a broader time range to capture long-term trends and cyclical changes. Additionally, an in-depth analysis of driving factors at different time points could reveal key turning points in the process of karst rocky desertification and potential opportunities for intervention.

4.2. Research Findings

From the research results, rocky desertification in Qujing City is primarily characterized by non-rocky desertification and potential rocky desertification. Most of the typical rocky desertification areas exhibit mild to moderate levels, with mild rocky desertification areas accounting for over 73%, while severely or extremely severely rocky desertified areas constitute less than 5%. The overall distribution shows a "south-light, north-heavy" pattern, which is consistent with results from other related studies [32]. The rocky desertification report of Yunnan Province (karst region) states that the rocky desertified area in Qujing City is 4267 km^2, while this study calculated the rocky desertified area as 4133.20 km^2 for the year 2016. The similarity in results indicates that the method of extracting the distribution of rocky desertification levels using decision tree classification based on vegetation cover, rock exposure rate, and slope in large-scale regional rocky desertification monitoring is both feasible and accurate.

In the study of driving factors, the primary drivers of rocky desertification in Qujing City were identified as vegetation cover, land use type, slope, and land reclamation rate. These findings align with those of similar studies [33], collectively affirming the significant relationships between vegetation cover, land use type, slope, land reclamation rate, and the occurrence of rocky desertification. In contrast to some studies in other regions where factors such as cultivated land area, population density, and per capita GDP were identified as major driving forces [1,3,29], this research highlights a larger contribution of natural environmental factors compared to socio-economic factors in the spatial distribution of rocky desertification. This suggests that the development and evolution of rocky desertification are not only associated with the fragile karst ecological geological background, but also influenced by the socio-economic development status, prevailing policies, and the natural environment during different periods. The varied causes of rocky desertification in different regions emphasize the need for tailored policies in rocky desertification control based on specific circumstances.

4.3. Policy Recommendations and Future Research

In addressing the primary driving factors of rocky desertification in Qujing City, comprehensive management strategies should be implemented. This includes enhancing vegetation cover by actively implementing policies such as the Natural Forest Resource Protection Project and compensation for forest ecological benefits, with a focus on protecting vegetation in rocky desertification-prone areas. To effectively alter the steep slope

cultivation conditions, agricultural measures such as conservation tillage, terrace construction, and small-scale water conservation projects should be adopted. The promotion of urbanization, accelerated migration of rural populations in karst areas, and advancement of various ecological restoration projects, such as protective afforestation, afforestation subsidies, and returning farmland to forest and grassland, are essential. The fundamental cause of the rocky desertification of land lies in excessive population density, far beyond the ecologically sustainable carrying capacity of karst land. Urbanization facilitates the transfer of surplus rural labor and population from karst areas, reducing the dependence on karst land and promoting the ecological restoration of rocky desertified land.

Consequently, the results demonstrate that the GEE cloud platform has great advantages in change monitoring research at large scales and in long time series. Remarkably, it is feasible and necessary to utilize the GEE cloud platform and geo-detector-assisted remote sensing monitoring technology to monitor and investigate the status of rocky desertification in Qujing City, Yunnan Province. In the future, the utilization of the GEE cloud platform can better assist scientific research.

5. Conclusions

In this study, based on Landsat5, Landsat8, and DEM data on Qujing City, Yunnan Province, the FVC, rock exposure rate, and slope were extracted utilizing the GEE cloud platform for the years of 1990, 1995, 2000, 2006, 2011, 2016, and 2020. The hierarchical classification of rocky desertification was carried out through decision trees, and a rocky desertification hierarchy map of Qujing City from 1990 to 2020 was drawn. Further, 11 direct or indirect driving factors related to rocky desertification were selected from natural environment and socio-economic aspects. Based on an analysis of the geographical probe method, the driving factors related to the spatial distribution of rocky desertification in Qujing City in 2000 were explored. The achieved conclusions are as follows:

(1) The degree of rocky desertification in Qujing City is relatively light, which is mainly dominated by no rocky desertification and potential rocky desertification. In general, most of the rocky desertification areas are mildly and moderately rocky desertification, with more than 73% of the area being mildly rocky desertified and less than 5% being severely or very severely rocky desertified. From 1990 to 2020, the area of rocky desertification decreased by 1728.38 km^2, while the area without rocky desertification increased by 1936.61 km^2, indicating that the rocky desertification in Qujing City had significantly improved.

(2) The main driving factors of rocky desertification in Qujing City are FVC (q = 0.41), land use type (q = 0.26), slope (q = 0.21), and the land reclamation rate (q = 0.21). Among them, the contribution rate of natural environmental factors to the spatial distribution of rocky desertification is greater than that of socio-economic factors. Areas with medium and low FVC (<0.7), with a low slope (0–8°) or high slope (35–80°), where the land type is cultivated land or grassland, and where the land reclamation rate is 10–70% are more prone to rocky desertification.

(3) The spatial distribution of rocky desertification varies significantly in the combination of main driving factors. FVC ∩ slope (q = 0.79) and slope ∩ land use type (q = 0.56) are the two interactive driving factors with a strong contribution rate to rocky desertification.

Author Contributions: W.G. and X.Y. designed the study. S.Z. collected the experimental data. W.G. wrote the paper. X.Y. revised the paper. All authors have read and agreed to the published version of the manuscript.

Funding: This research was supported by the Yunnan Provincial Government under the "Xingdian Talent Support Program" Youth Talent Program (grant number XDYC-QNRC-2022-0251).

Institutional Review Board Statement: Not applicable.

Informed Consent Statement: Not applicable.

Data Availability Statement: Data are contained within the article.

Conflicts of Interest: The authors declare that the research was conducted in the absence of any commercial or financial relationships that could be construed as potential conflicts of interest.

References

1. Chong, G.; Hai, Y.; Zheng, H.; Xu, W.; Ouyang, Z. Characteristics of changes in karst rocky desertification in Southtern and Western China and driving mechanisms. China. *Geogr. Sci.* **2021**, *31*, 1082–1096. [CrossRef]
2. Dai, Q.H.; Peng, X.D.; Yang, Z.; Zhao, L.S. Runoff and erosion processes on bare slopes in the karst rocky desertification area. *Catena* **2017**, *152*, 218–226. [CrossRef]
3. Ying, B.; Xiao, S.-Z.; Xiong, K.-N.; Cheng, Q.-W.; Luo, J.-S. Comparative studies of the distribution characteristics of rocky desertification and land use/land cover classes in typical areas of Guizhou province, China. *Environ. Earth Sci.* **2014**, *71*, 631–645. [CrossRef]
4. Chen, S.T.; Guo, B.; Zhang, R.; Zang, W.Q.; Wei, C.X.; Wu, H.W.; Yang, X.; Zhen, X.Y.; Li, X.; Zhang, D.F.; et al. Quantitatively determine the dominant driving factors of the spatial–temporal changes of vegetation NPP in the Hengduan mountain area during 2000–2015. *J. Mt. Sci.* **2021**, *18*, 427–445. [CrossRef]
5. Xiong, Y.J.; Qiu, G.Y.; Mo, D.K.; Lin, H.; Sun, H.; Wang, Q.X.; Zhao, S.H.; Yin, J. Rocky desertification and its causes in karst areas: A case study in Yongshun county, Hunan province, China. *Environ. Geol.* **2009**, *57*, 1481–1488. [CrossRef]
6. Gao, J.B.; Wang, H. Temporal analysis on quantitative attribution of karst soil erosion: A case study of a peak-cluster depression basin in Southwest China. *Catena* **2019**, *172*, 369–377. [CrossRef]
7. Zhang, Y.Q.; Liao, J.; Long, Y.; An, J.; Xu, S.J.; Wang, X.L. Dating reservoir deposits to reconstruct sediment yields from a small limestone catchment in the Yimeng Mountain region, China. *Catena* **2018**, *166*, 1–9. [CrossRef]
8. Zhong, S.F.; Li, Y.H.; Wu, C.H.; Lu, W.P.; Yang, X. TM and ETM image based monitoring on rocky desertification in region of the return farmland pasture or forest in Tiandong county Guangxi province, China. *Sens. Lett.* **2012**, *10*, 301–308. [CrossRef]
9. Zhou, Z.F. Application of remote sensing and GIS technology for land desertification in Guizhou karst region. *Bull. Soil Water Conserv.* **2001**, *21*, 52–54.
10. Li, W.H.; Yu, D.Q. A Study of the technology for remote sensing investgaion of rocky desertificattion in areas of karstt sony hiloss. *Remote Sens. Land Resour.* **2002**, *1*, 34–37.
11. Cao, J.J.; Wen, X.G.; Zhang, M.M.; Luo, D.Y.; Tan, Y. Information extraction and prediction of rocky desertification based on remote sensing data. *Sustainability* **2022**, *14*, 13385. [CrossRef]
12. Chong, G.S.; Hai, Y.; Zheng, H.; Xu, W.H.; Ouyang, Z.Y. Progresses in remote sensing information extraction methods for rocky desertification. *J. Appl. Sci.* **2021**, *39*, 961–968.
13. Wang, H.; Wang, Y.Y.; Cai, H.; Jia, Y.; Zhou, Q. Research on temporal and spatial changes of multi-scale rocky desertification based on multi-source data. Chin. *J. Undergr. Space Eng.* **2021**, *17*, 1044–1050.
14. Li, W.; Wei, M. Study on monitoring rocky desertification based on the combination of remote sensing interpretation and geographical conditions. *Bull. Surv. Mapp.* **2020**, *2*, 121–125.
15. Wang, J.F.; Hu, Y. Environmental health risk detection with GeogDetector. *Environ. Model Softw.* **2012**, *33*, 114–115. [CrossRef]
16. Bai, X.Y.; Wang, S.J.; Xiong, K.N. Assessing spatial-temporal evolution processes of karst rocky desertification land: Indications for restoration strategies. *Land Degrad. Dev.* **2013**, *24*, 47–56. [CrossRef]
17. Chen, Y.L.; Mo, J.F.; Mo, W.H. Temporal and spatial distributions of rocky desertifi-cation in Guangxi karst area in the past 30 Years. *Guangxi Sci.* **2018**, *25*, 625–631.
18. Wang, S.J.; Liu, Q.M.; Zhang, D.F. Karst rocky desertification in southwestern China: Geomorphology, landuse, impact and rehabilitation. *Land Degrad. Dev.* **2004**, *15*, 115–121. [CrossRef]
19. Sheng, M.; Xiong, K.; Wang, L.; Li, X.; Li, R.; Tian, X. Response of soil physical and chemical properties to Rocky desertification succession in South China Karst. *Carbonates Evaporites* **2018**, *33*, 15–28. [CrossRef]
20. Zhang, X.-B.; Bai, X.-Y.; He, X.-B. Soil creeping in the weathering crust of carbonate rocks and underground soil losses in the karst mountain areas of southwest china. *Carbonates Evaporites* **2011**, *26*, 149–153. [CrossRef]
21. Xi, H.P.; Wang, S.J.; Bai, X.Y. Spatio-temporal characteristics of rocky desertification in typical karst areas of Southwest China: A case study of Puding County, Guizhou Province. *Acta Ecol. Sin.* **2018**, *38*, 8919–8933.
22. Khalid, M.; Tan, H.X.; Ali, M.; Rehman, A.; Liu, X.X.; Su, L.T. Karst rocky desertification diverged the soil residing and the active ectomycorrhizal fungal communities thereby fostering distinctive extramatrical mycelia. *Sci. Total Environ.* **2022**, *807*, 151016. [CrossRef]
23. Lan, G.Y.; Liu, C.; Wang, H.; Cao, J.H.; Tang, W.; Li, Q. Linking soil redistribution to soil organic carbon using 210Pbex along different complex toposequences in a karst region, southwest China. *Catena* **2021**, *202*, 105239. [CrossRef]
24. Zheng, X.; Fu, J.; Ramamonjisoa, N.; Zhu, W.; He, C.; Lu, C. Relationship between wetland plant communities and environmental factors in the tumen river basin in Northeast China. *Sustainability* **2019**, *11*, 1559. [CrossRef]
25. Jiang, Y.; Gao, J.B.; Yang, L.; Wu, S.H.; Dai, E.F. The interactive effects of elevation, precipitation and lithology on karst rainfall and runoff erosivity. *Catena* **2021**, *207*, 105588. [CrossRef]
26. Zhang, X.L.; Gan, S. Research on extracting rocky desertification information based on NDRI dimidiate pixel model. *New Process* **2014**, *1*, 72–75.

27. Xu, G.Y.; Xiao, J.; Oliver, D.M.; Yang, Z.Q.; Xiong, K.N.; Zhao, Z.M. Spatio-temporal characteristics and determinants of anthropogenic nitrogen and phosphorus inputs in an ecologically fragile karst basin: Environmental responses and management strategies. *Ecol. Indic.* **2021**, *133*, 108453. [CrossRef]
28. Yan, T.T.; Xue, J.H.; Zhou, Z.D.; Wu, Y.B. Effects of biochar-based fertilizer on soil bacterial network structure in a karst mountainous area. *Catena* **2021**, *206*, 105535. [CrossRef]
29. Wang, M.M.; Wang, S.J.; Bai, X.Y.; Li, S.J.; Li, H.W.; Cao, Y.; Xi, H.P. Evolution characteristics of karst rocky desertification in typical small watershed and the key characterization factor and driving factor. *Acta Ecol. Sin.* **2019**, *39*, 6083–6097.
30. Wang, J.F.; Xu, C.D. Geodetector: Principle and prospecttive. *J. Geogr.* **2017**, *72*, 116–134.
31. Yin, H.; Ziang, Z.C.; Luo, W.Q. Research on the dynamic evaluation of water and soil Loss and rock desertification in karst regions in Southwestern China. *Res. Soil Water Conserv.* **2011**, *18*, 66–70.
32. Lu, T.; Hu, W.Y.; Zhang, J. Spatial and temporal evolution of rocky desertification in karst area of eastern Yunnan: A case study of Qujing City. *J. Arid Land Resour. Environ.* **2021**, *35*, 71–79.
33. Lu, T.; Zhang, J.; Hu, W.Y. Spatio-temporal evolution and driving mechanism of rocky desertification in eastern karst area. *J. Ecol. Rural Environ.* **2022**, *38*, 418–427.